Chapter 14

ULTRACOMPACT OPTICAL SENSORS BASED ON HIGH INDEX-CONTRAST PHOTONIC STRUCTURES

Alfred Driessen, Hugo J.W.M. Hoekstra, Wico Hopman, Henry Kelderman, Paul V. Lambeck, Joris van Lith, Dion J.W. Klunder, René M. de Ridder
Integrated Optics MicroSystems, MESA+
University of Twente
P.O. Box 217
7500 AE Enschede, The Netherlands

Evgeni Krioukov and Cees Otto
Biophysical Techniques Group, MESA+
University of Twente
P.O. Box 217
7500 AE Enschede, The Netherlands

1. INTRODUCTION

There is a strong parallelism between electronic integrated circuits (ICs) and integrated optics. In both cases micro- and increasingly nano-technology is applied resulting in devices for a broad spectrum of applications: communication, data processing, sensing and others. The most striking difference is the maturity and complexity. Electronic ICs have followed Moore's law for about 40 years resulting in the currently more than 100 million transistors in a single chip, whereas in photonic circuitries 10 – 100 functional elements per chip represent state-of-the-art results. Photonics in this respect is clearly lagging behind and will do so also in future, as the minimum dimensions of the functional elements will be always in the order of the wavelength of light, i.e. at least some hundreds of nm. But even then, a density of 10^3 to 10^5 functional elements per optical chip is feasible, so that the term Very Large Scale Integrated (VLSI) photonics[1] is not an exaggeration.

Optical circuits will not simple mimic electronics, but will exploit in a complementary way the unique phenomena offered by light. For example THz bandwidth amplification is straightforward in optical structures with

F. Baldini et al. (eds.), Optical Chemical Sensors, 281–295.

gain, e.g. semiconductors or rare-earth doped dielectric waveguides. In electronics this is impossible even in a medium term future. In the case of sensors, optical phenomena can be exploited in highly sensitive and selective devices. In this contribution we will discuss how ultra-compact integrated optics or VLSI photonics could play a role in optical sensing. For this aim we summarize first some basic properties of integrated optics concentrating thereby on optical microresonators and more general on nanophotonics. Thereafter we review some recent results of high index-contrast optical sensors. In the following section we discuss the severe challenges for low-cost mass production of complex nanophotonic sensor systems. Finally some conclusions are presented.

2. BASIC PROPERTIES OF HIGH INDEX-CONTRAST WAVEGUIDING STRUCTURES

Optical waveguiding occurs when light is confined in 1 (slab waveguide), 2 (channel waveguide) or 3 (resonator) dimensions. Wave propagation can be understood by the ray-picture, see Figure 1a, or as propagation of modes according to Maxwell's equation, Figure 1b. If two waveguides run parallel with each other at a small distance so that one mode feels the index distortion by the second waveguide, mode coupling can occur with consequently power exchange, Figure 1c. At curved surfaces special modes can occur that reflect only at the outer rim of the waveguiding structure, so called whispering gallery modes, Figure 1d. The confinement originates from total reflection at dielectric interfaces (index guiding) or, in the case of photonic bandgap (PBG) structures, from Bragg reflection at periodic index variations. In both cases, with appropriate high index-contrast materials, the extension of the modal fields can be reduced well below the micrometer range.

Special attention has to be given to low-loss bends, which for decreasing bend radius ask for increasing index contrast Δn. The minimum bend radius

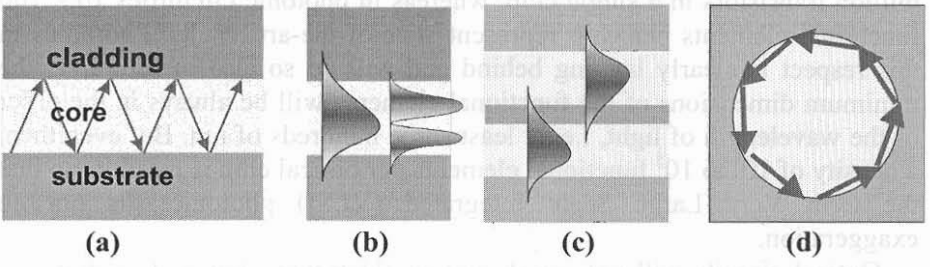

Figure 1. Schematic illustration of waveguiding structures. a: ray-picture; b: modal intensity distribution obtained with the aid of Maxwell's equation; c: mode coupling; c: whispering gallery mode.

for waveguides with modes that are matched to standard single mode fiber ($\Delta n \sim 0.01$), is about 5mm. It is obvious that no complex optical circuitry can be built with such a large radius. For high Δn, the radius can be reduced to a few micrometers. In this way compact structures with optical feedback become possible that allow for a large variety of optical functions. It is interesting to note that increased density and complexity leading eventually to VLSI photonics ask for high index-contrast and consequently submicron waveguides, which can truly be classified as nanophotonics. In both approaches, index guiding or PBG structures, the devices may have the same overall dimensions. Index guiding is an evolutionary approach, as Δn can gradually be increased, whereas the latter is rather revolutionary as the starting point is an ultra-high index contrast $\Delta n > 1$.

An optical microresonator[2-4] is an integrated optics structure with optical feedback that allows a variety of functions like wavelength filtering, optical switching or optical sensing. Figure 2a gives a top view of such a device with two adjacent single mode port waveguides. Light enters at I_{in} and couples in part to the resonator. The rest of the power goes to $I_{through}$. Within the ring light propagates in a whispering gallery mode and couples partly to the output waveguide I_{drop}. After further propagation the light couples partly to $I_{through}$. Depending on the phase of the light after a roundtrip, constructive or destructive interference will occur between the just entering and the already present beam within the ring and also between the beam coupled out to $I_{through}$ and the just transmitted beam. In the case of constructive interference the resonator is on-resonance resulting in a largely enhanced intensity within the ring. In that case the light coupled to $I_{through}$ has a phase shift of 180° with respect to the just transmitted beam. In this way the transmitted intensity can be largely reduced, in loss-less resonators with symmetric couplers even to zero. Figure 2 b gives schematically the resulting normalized spectral response of such a resonator to a constant power input signal with changing wavelength or alternatively changing

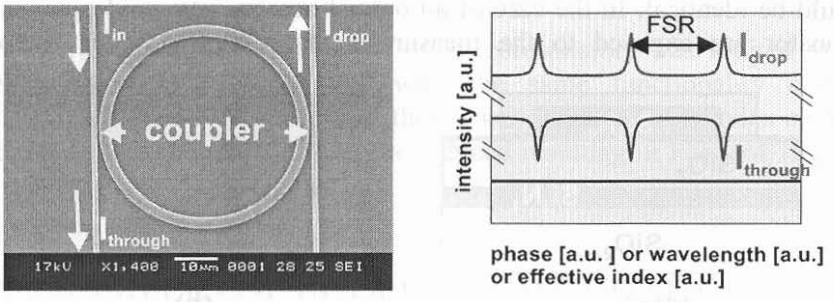

Figure 2. Microresonator with two adjacent waveguides serving as in- and output port; (a): top view; (b): schematic spectral response to a constant input intensity (FSR: free spectral range).

phase in the resonator or changing effective index. The power $I_{through}$ is always equal to I_{in} with exception near to the resonance, in that case $I_{drop} = I_{in}$.

The performance of the microresonator is characterized by the free spectral range (FSR) and the 3dB bandwidth $\Delta\lambda_{3dB}$ of the resonance peaks. With increasing ring losses, the FSR will decrease and $\Delta\lambda_{3dB}$ will increase. A relative measure for the wavelength selectivity of the resonator is the finesse F = FSR/ $\Delta\lambda_{3dB}$. Other parameters are the quality factor $Q = \lambda/\Delta\lambda_{3dB}$, the cavity ring-down time $\tau_{cav} = \lambda\, Q/2\pi c$ and the average number of roundtrips of photons in a resonator $m = F/2\pi$. For the design of a microresonator the field coupling constant κ between the port waveguides and the ringresonator plays an essential role. In a loss-less resonator with an infinite unloaded finesse the only load is induced by coupling to the port waveguides. Large effective coupling can only be obtained by proper phase matching between the modes in the ring and port waveguides.

There are principally two solutions for the positioning of the adjacent waveguides with respect to the resonator: horizontal or vertical arrangement. Figure 3 gives schematically the geometries. In the vertical arrangement (Figure 3a), a two-step lithographic process is needed. The coupling constant is mainly determined by the thickness and refractive index of the intermediate layer and the relative lateral offset of the underlying waveguide with respect to the ring. This approach provides also design freedom for an independent optimization for ring and port waveguides. Due to the vertical stacking only the resonator itself is exposed to the measurand in the case of sensing applications, the port waveguides are shielded by the separation layer.

In the case of horizontal coupling (Figure 3b), only a single lithographic step with a single mask is needed. The coupling is mainly determined by the width w of the gap between the straight and bent waveguides and demands nanometer precision in the case of high refractive index contrasts. In addition, there is reduced design flexibility as core layer and core thickness should be identical. In the case of an optical sensor, waveguides as well as resonator are exposed to the measurand. Its refractive index not only

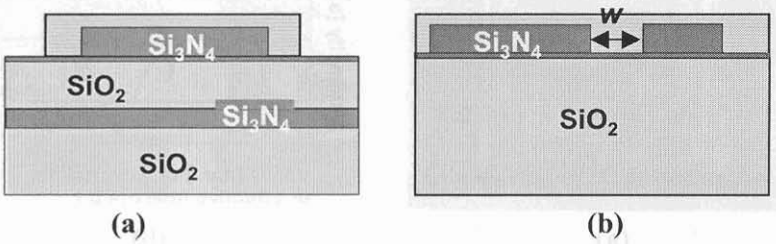

Figure 3. Cross section of the two basic geometries for microresonators with port waveguides; (a) vertical arrangement; (b) lateral arrangement (the dashed region indicates the analyte layer). The structure in this case is fabricated in silicon-based technology, with the index of refraction of SiO_2 and Si_3N_4 1.45 and 2.0 respectively.

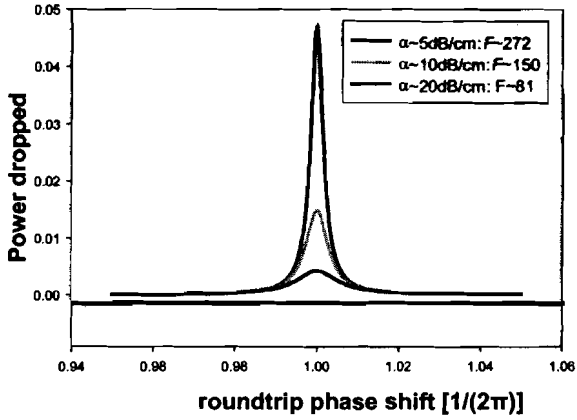

Figure 4. The drop power of a microresonator as a function of phase shift for different values of roundtrip losses α, c.q finesse *F*.

influences the effective index of the ring and port waveguide modes, but also the coupling constant.

In Figure 2b the spectral response of a microresonator as a function of wavelength has already been given. Just by changing the wavelength, the effective index or the phase light can be directed either to the drop or the through port. When used as a refractive sensor the effective index change of the ring mode is a measure of the concentration or amount of the desired quantity. Small changes near the inversion points of the resonance slopes will lead to large intensity variations at the through as well as drop port. There is another sensing mode. If one considers a single resonance line, the amplitude and width is determined by the roundtrip losses, see Figure 4. By changing the losses and consequently reducing the Q-factor, light can effectively be switched between the two drop ports.

The microresonator therefore can also be used as a sensitive absorption sensor. In both set-ups as refractive or absorption sensor, the ultimate sensitivity is determined by the slope of the resonance peak, which is related to the resonator losses.

In the foregoing the description of microresonators was limited to the index guiding type. Resonators with the same functionality can be implemented in PBG structures[5]. In these cases, with the high index contrast used, the cavity volume is even more reduced resulting in FSRs of 10 - 100 nm.

3. EXAMPLES OF ULTRACOMPACT OPTICAL SENSORS

Optical sensing in general is based on changes of the optical properties of materials within the optical circuitry due to changes in the environment.

Except for light generating sensors (e.g. based on luminescence), most optical sensors operate by detecting changes in the refractive index or the absorption at a certain wavelength. Using interferometric sensors, changes as low as 10^{-8} in the index of refraction can be measured[6]. Optical microresonators, based on high index-contrast structures, offer some unique properties for optical sensing as they are very sensitive to small changes in the refractive index. In addition, they are very small (chip area less than 0.01 mm^2) and the measuring volume can be below 1 pL (10^{-12} L). For this reason, they are ideally suited for Lab-on-a-chip applications and sensor arrays that in combination with advanced data read-out could be used as optical nose or tongue.

Krioukov et al.[7] demonstrated the feasibility of optical sensing by measuring the wavelength dependence of the scattered light of a microresonator that is proportional to the light power inside the resonator. For a practical design the change in resonance intensity could much easier be detected by measuring directly the light intensity at the drop port. The device has been realized in SiO_xN_y technology[8] in a vertical coupling geometry. Figure 5 gives a schematic cross-section and top view of the device with a radius of 15 μm. Also the approximate mode profile of the whispering gallery mode is given, which extends into the analyte layer.

For a proof of principle they immersed the microresonator in glucose solutions of various concentrations and measured the scattered light when light from a tunable laser was fed to the input waveguide. Figure 6 gives the experimental resonant curves for pure water and a 0.5 and 1% glucose solution. In the not yet optimized set-up refractive index changes well below 10^{-4} could be detected.

Figure 6b gives an overview of the experimental wavelength shift for glucose solutions and ethanol with respect to water, indicating the feasibility of a large measuring range together with high resolution. Large improvements can be obtained by working with even higher finesse resonators and advanced curve fitting. Ultimately a detection limit of index changes as low as 10^{-8} should be feasible.

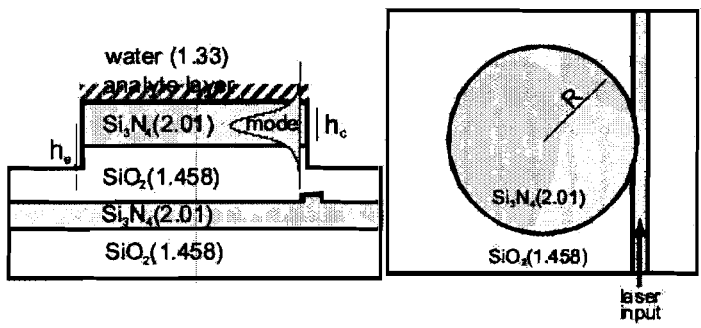

Figure 5. Cross section (a) and top view (b) of an integrated optical microresonator sensor with radius R = 15 μm.

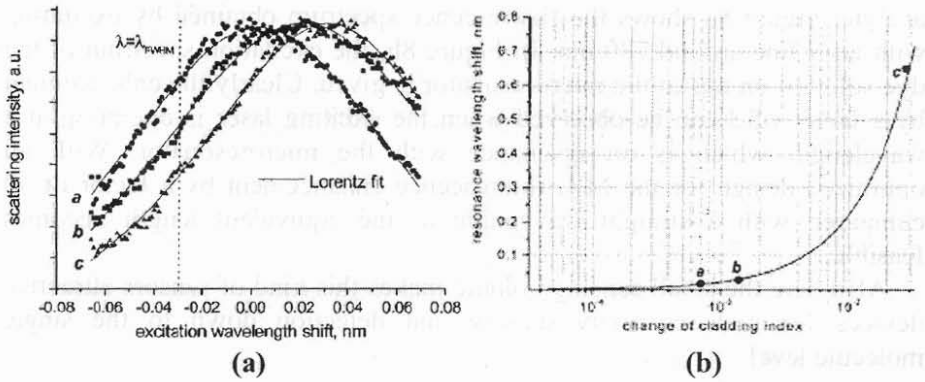

Figure 6. Experimental results of Krioukov et al.[7] of microresonator based optical sensing of glucose; (a) scattering spectra near a resonance recorded by fine laser tuning for "a" water, "b" 0.5% glucose and "c" 1% glucose in the cladding; (c): measured shifts in resonance wavelength for three claddings for "a" 0.5 % glucose, "b" 1% glucose and "c" EtOH (n = 1.36).

Recently Chao and Gua[9] employed polymer microrings with sharp asymmetrical resonance for measuring glucose solutions. They found a detection limit of 24 mg/dl corresponding to a 3 x 10^{-5} index change.

In a second paper Krioukov et al.[10] demonstrated the use of optical microresonators for enhanced optical spectroscopy and sensing. They employed a similar device as depicted in Figure 5, with water as the cladding layer. Measuring the scattering as function of wavelength, a large enhancement of the scattered power at the resonance wavelengths could be observed, see Figure 7. In order to probe more specifically the fluorescence enhancement an Indocyanine Green dye (10^{-5} M in water) was used as

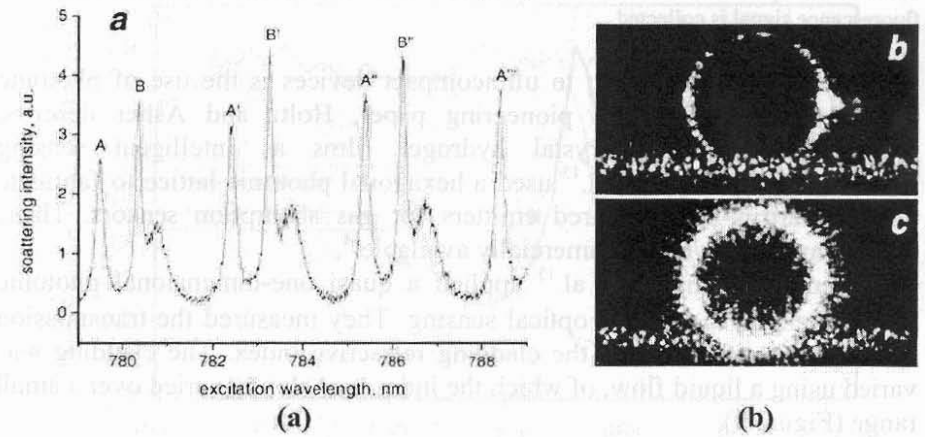

Figure 7. Light scattering of a microresonator with a water cladding; (a) spectra obtained as response to a tunable laser with clearly visible high finesse resonances; (b) CCD camera images of the microresonator obtained off-resonance, (c) idem on-resonance.

analyte. Figure 8a shows the fluorescence spectrum obtained by excitation with laser line around 780 nm. In Figure 8b, the excitation spectrum of the dye solution on top of the microresonator is given. Clearly the enhancement by a factor of 3 can be observed when the exciting laser is operating at a wavelength which is on resonance with the microresonator. With an optimized design for the MR, fluorescence enhancement by a factor of 40 compared with a straight waveguide of the equivalent length becomes feasible.

Also here the small sensing volume makes this kind of sensors attractive devices for high-sensitivity sensing and detection down to the single molecule level.

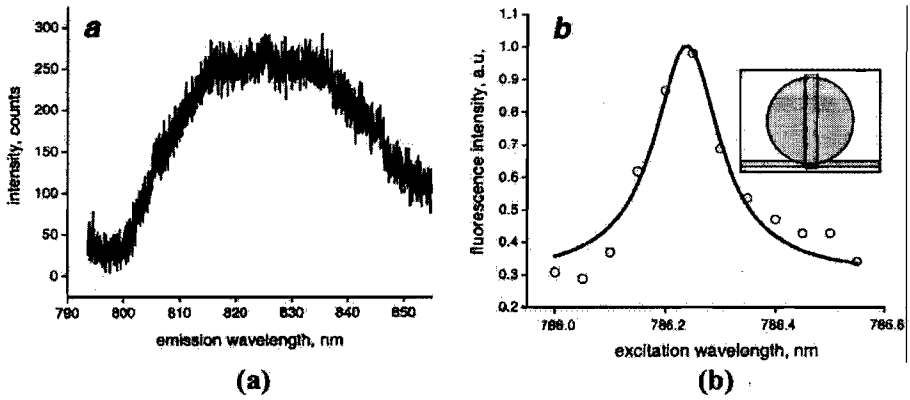

Figure 8. Optical spectroscopy of a indocyanine green dye solution (10^{-5} M in water); (a): fluorescence spectrum obtained by excitation around 780 nm; (b): excitation spectrum obtained on top of a microresonator; the rectangle in the inset shows the area from which the fluorescence signal is collected.

An alternative approach to ultracompact devices is the use of photonic crystals structures[11]. In a pioneering paper, Holtz and Asher describe polymerized colloidal crystal hydrogel films as intelligent sensing materials[12]. El-Kady and al.[13] used a hexagonal photonic lattice to fabricate tunable narrow-band infrared emitters for gas absorption sensors. These sensors are meanwhile commercially available[14].

Recently Hopman and al.[15] applied a quasi one-dimensional photonic crystal (length 76 μm) for optical sensing. They measured the transmission spectrum as a function of the cladding refractive index. The cladding was varied using a liquid flow, of which the index was slowly varied over a small range (Figure 9).

An increase of the cladding refractive index causes a shift of the transmission spectrum of the grating towards longer wavelengths of approximately 23 nm per unit index change (Figure 10). The steep slopes of the photonic band edges (in our case especially the dielectric band edge - at

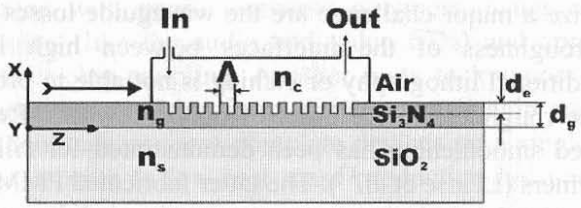

Figure 9. Cross-section of a refractive index sensor based on a quasi one-dimensional photonic crystal with grating period Λ = 190 nm. The top cladding over the grating is formed by a fluid contained in a cuvette that is sealed to the sensor chip.

the long-wavelength side of the gap) can be used for increasing the sensitivity of the device.

With a simple photodetector, a variation of 4×10^{-4} in the cladding index could be detected. With some straightforward optimization, an improvement of the resolution by two orders of magnitude may be feasible. A thermally induced spectral shift of approximately 8 pm/K was observed.

4. CHALLENGES FOR NANOPHOTONIC SENSORS

In the previous section first results with promising nanophotonic sensor devices have been demonstrated. It is still some work needed before low-cost, high sensitive and complex optical sensors with a large number of optical functions will be available. For the increase in sensitivity and

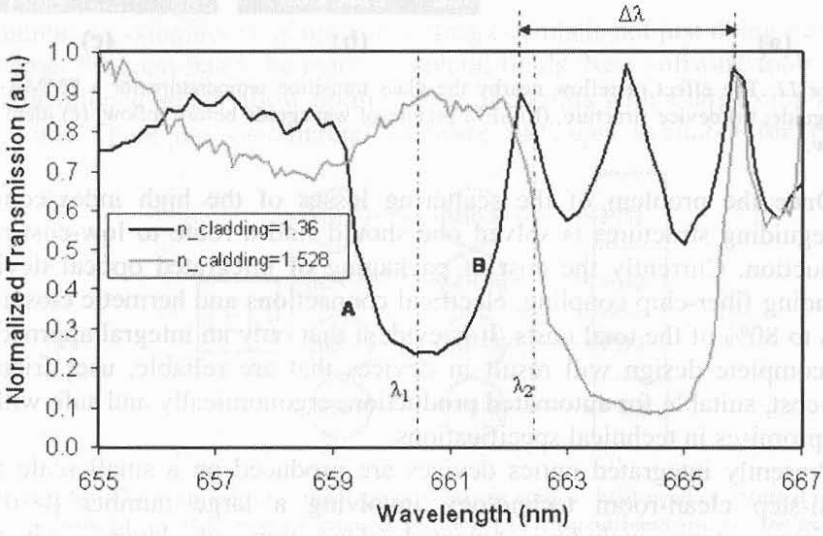

Figure 10. Normalized transmission spectra for two different cladding indices. The air band edge and the dielectric band edge are labeled with the letters A and B.

reduction in size a major challenge are the waveguide losses mainly due to the surface roughness of the interfaces between high index contrast materials. Traditional lithography or etching is not able to provide solutions for an ultimate roughness in the order of only a few nm. Recently surface tension induced smoothening has been demonstrated for silica (Armani et al.[16]) and polymers (Leinse et al.[17]). The latter fabricated PMMA waveguides with dispersive red-1 sidechains by conventional lithography and RIE etching (see Figure 11a). The waveguide losses at 1550 nm were measured by launching a laser in a spiral waveguide of 3.5 cm length and taking an image with an IR- sensitive CCD camera. Heating the waveguide for two hours at 135 °C allowed reflowing of the material and surface smoothening, see Figures 11b and 11c. The effect of the smoothening was a reduction of waveguide losses from 3 dB/cm to 1 dB/cm. Taking into account the materials losses, about 0.8 dB/cm as measured separately in slab waveguides, the scattering losses could be reduced to about 0.2 dB/cm.

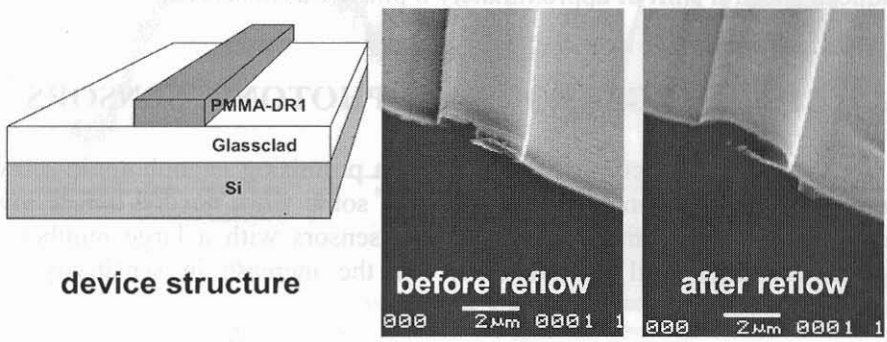

Figure 11. The effect of reflow nearby the glass transition temperature for a PMMA-DR1 waveguide; (a) device structure, (b) SEM picture of waveguide before reflow, (c) idem after reflow.

Once the problem of the scattering losses of the high index-contrast waveguiding structures is solved one should find a route to low-cost mass production. Currently the cost of packaging of integrated optical devices, including fiber-chip coupling, electrical connections and hermetic closure, is 60% to 80% of the total costs. It is evident that only an integral approach to the complete design will result in devices that are reliable, user friendly, low-cost, suitable for automated production, ergonomically and safe without compromises in technical specifications.

Presently integrated optics devices are produced on a small scale by a multi-step clean-room technology involving a large number (>30) of precision steps including repeated deposition of layers, advanced lithography, etching and finally fiber-chip coupling and bonding. To avoid this inherently expensive processing simple fabrication techniques have to be

used like working with photo definable polymers, using high precision molding techniques (like the audio and video CDs) and applying passive alignment for fiber-chip coupling. Another route to low-cost production is further miniaturization resulting in an extreme small chip area that allows integration of thousands or more complete devices on a single wafer. With both approaches a route to low-cost mass production becomes feasible so that on a longer term complex disposable optical sensors will become possible.

Finally there is the challenge of complexity, which enters if one would like to quit from expensive external optical measuring apparatus like tunable light sources, spectrometers and sensitive detector arrays. This is possible if the optical sensor itself incorporates these optical functions. Consider, for example, a sensor chip where microresonators with the typical wavelength response as depicted in Figure 2b are employed as wavelength filter together with a set of microresonators as sensors (see Figure 12). In this case, a cheap broadband light source like a LED could be used together with silicon photodiodes fabricated in CMOS technology. An additional advantage is the inherent possibility for temperature compensation, as only one of the microresonators for each wavelength is exposed to the measurand.

The complexity increases even more if one starts incorporating multisensor functions, Figure 13. Even if for improved performance the filter elements would consist of cascaded microresonators selecting 8 wavelengths, the complete multi-sensor with 96 microresonators could still fit on a few mm^2. In this way an optical nose or optical tongue with only a modest power supply and without optical peripheral equipment would become feasible.

Increasing complexity of optical sensing circuits is not just doing more of the same. Progress has to be made in several fields. New software tools have to be developed which allow optimization of circuits with a large number of functions. There are commercial software packages available for single

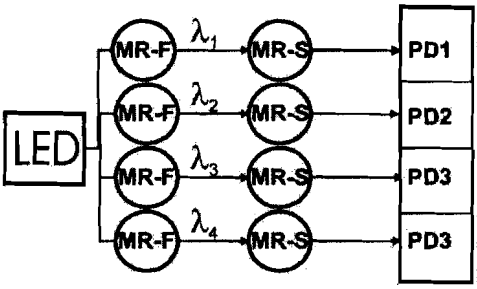

Figure 12. Schematic lay-out of compact optical sensor chip without need of external optical apparatus with identical microresonators as sensors; LED: broad band source, for example Light Emitting Diode, MR-F: microresonator used as optical filter, MR-S: microresonator used as optical sensor, PD: Photo Diode.

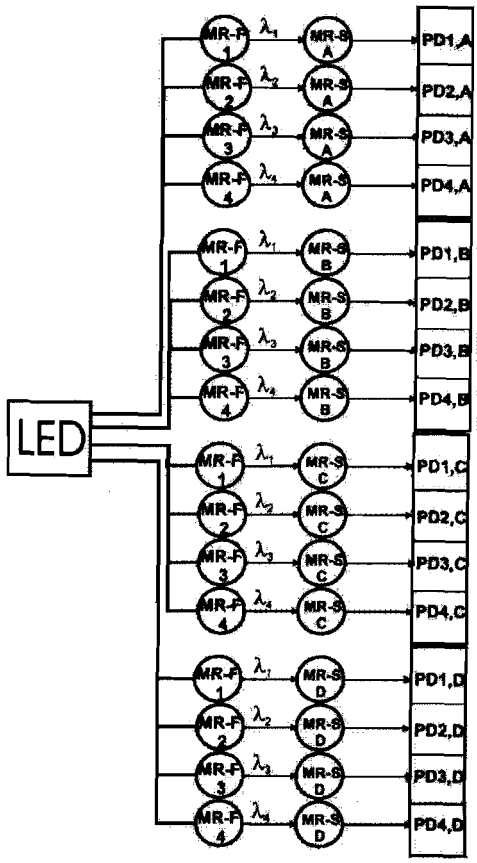

Figure 13. Schematic lay-out of compact optical sensor chip without need of external optical apparatus with 4 different sets of sensing arrays.; LED: broad band source, for example Light Emitting Diode, MR-F: microresonator used as optical filter, MR-S: microresonator used as optical sensor, PD: Photo Diode.

elements, but in contrast to electronic IC design, not for complete integrated optical systems. In addition, the technology has to be improved with respect to accuracy, uniformity, reproducibility and yield. For a single element circuit a yield of 80% is acceptable, for an 8 element circuit this would result in a yield of 17% and for 16 elements in 3%, which is becoming unrealistic small even for just demonstration purposes.

Increasing complexity means also reducing size. The devices described in the previous section had approximately a sensitive area of 10^2 to 10^3 μm^2. Assuming an evanescent field penetrating 1 μm into the measurand, the measuring volume is 10^2 to 10^3 μm^3, i.e. 0.1 to 1 pL. Increasing the index contrast a measuring volume in the range of fL becomes feasible without loss in sensitivity. In this way the route to highly integrated lab-on-a-chip devices becomes practical. One also can speculate on single molecule detection or single molecule counters.

What would be the target in 10 to 20 years? A recent EC report "Vision 2020 Nanoelectronics at the Centre of Change"[18] identifies 7 items where nanosciences and nano-materials offer breakthrough applications; two of them deal explicitly with sensors:

- nanophotonics - will still increase the speed and lower the cost of data transmission, and also have important applications in sensor technology;
- nano-sensors and nano-actuators - more sensitive and selective sensors and actuators will accommodate voice, vision and tactile senses and stimulation, as well as offering new applications such as biometrics and environmental monitoring.

5. CONCLUSIONS

In the foregoing the potential of integrated optical devices for sensing has been demonstrated and a view of present and future research has been given. A comparison with VLSI electronics has been made, but one has to bear in mind that optical circuitries have a delay of more than 30 years with respect to electronic ICs.

VLSI photonics is feasible by using high index-contrast waveguiding structures in microresonators and other advanced structures. The application fields include optical communication and optical sensing. Two approaches can be followed, index guiding with an evolutionary route to size reduction by increasing gradually the index contrast, and PBG structures, which from the very beginning apply ultra high index-contrast in ultra-compact structures. Both approaches make use of nanophotonic technology.

Severe challenges have to be faced to arrive eventually at low-cost, mass produced VLSI photonic sensors, among others: improved design software, integrated design, improved technology with excellent reproducibility, uniformity and yield with tight specifications and automated production and testing procedures, Once these have been achieved, optical sensors will become consumer photonics devices.

The progress in photonic circuits now and in the near future will be mainly driven by the needs of optical communication. Other application fields, like optical sensing, can take profit of the results obtained there and apply them to the own specific demands.

The introduction of low-cost, mass-produced optical nano-sensors will be based on multidisciplinary research where all aspects - photonics, micro- en nanotechnology, (bio-)chemistry of interfaces and system aspects - are considered. Real breakthrough therefore will be only possible in close cooperations between strong groups active in the different fields.

ACKNOWLEDGMENTS

The authors would like to thank Mart Diemeer, Anton Hollink, Arne Leinse, Gabriel Sengo, Freddy Tan, Henk van Wolferen and Kerstin Wörhoff for their contribution in the research described in this paper.

Financial support is acknowledged of the Dutch Science Foundations FOM, STW and BTS and the EC project NAIS.

REFERENCES

1. Little B.E., Chu S.T., Pan W., Kokubun Y., Microring resonator arrays for VLSI photonics, *IEEE Phot. Techn. Letters* 2000; 12: 323-325.
2. Klunder D.J.W., Krioukov E., Tan F.S., van der Veen T., Bulthuis H.F., Sengo G., Otto C., Hoekstra H.J.W.M.and Driessen A., Vertically and laterally waveguide-coupled cylindrical micro resonators in Si_3N_4 on SiO_2 technology, *Appl. Phys. B* 2001; 73: 603-608.
3. Klunder D.J.W., Photon Physics in Integrated Optics Microresonators, Ph.D. thesis, University of Twente, 135 p (2002).
4. Driessen A., Geuzebroek D.H., Hoekstra H.J.W.M., Kelderman H., Klein E.J., Klunder D.J., Roeloffzen C.H.G., Tan F.S., Krioukov E., Otto C., Gersen H., van Hulst N.F. and Kuipers L., Microresonators as building blocks for VLSI photonics, AIP Conf. Proc. 709, 1-18 (2004).
5. Akahane Y., Asano T., Song B.S. and Noda S., High-Q photonic nanocavity in a two-dimensional photonic crystal, *Nature* 2003; 425: 944-947.
6. Heideman R.G. and Lambeck P.V., Remote opto-chemical sensing with extreme sensitivity: design, fabrication and performance of a pigtailed integrated optical phase-modulated Mach-Zehnder interferometer system, *Sensors and Actuators B* 1999; 61: 100-127.
7. Krioukov E., Klunder D.J.W., Driessen A., Greve J., Otto C., *Optics Letters* 2002; 27: 512-514.
8. Wörhoff K., Hilderink L.T.H., Driessen A., and Lambeck P.V., Silicon oxynitride: a versatile material for integrated optics application, *J. Electrochem. Soc.* 2002; 149: 85-91.
9. Chao C-Y. and Guo L.J., Biochemical sensors based on polymer microrings with sharp asymmetrical resonance, *Appl. Phys. Letters* 2003; 83: 1527-1529.
10. Krioukov E., Klunder D.J.W., Driessen A., Greve J., Otto C., Integrated optical microcavities for enhanced evanescent-wave spectroscopy, *Optics Letters* 2002; 27: 1504-1506.
11. Prasad P.N., *Nanophotonics*, John Wiley, Hoboken, New Jersey (2004), pp 67 ff.
12. Holtz J.H. and Asher S.A., Polymerized colloidal crystal hydrogel films as intelligent chemical sensing materials, *Nature* 1997; 389: 829-832.
13. El-Kady, Biswas R., Ye Y., Su M.F., Puscasu I., Pralle M., Johnson E.A., Daly J. and Greenwald A, Tunable narrow-band infrared emitters from hexagonal lattices, *Photonics and Nanostructures* 2003; 1: 69-77.
14. See http://www.ion-optics.com/sensorchip.asp.
15. Hopman W., Pottier P., Yudistira D., van Lith J., Lambeck P.V., de la Rue R., Driessen A., Hoekstra H.J.W.M. and de Ridder R.M., Proc. ICTON 2004, Wroclaw, Poland, pp.342-345 (2004).
16. Armani D.K., Kippenberg T.J., Spillane S.M. and Vahala K.J., Ultra-high-Q toroid microcavity on a chip, *Nature* 2003; 421: 925-928.

17. Leinse A., Diemeer M.B.J. and Driessen A., Scattering loss reduction in polymer waveguides by reflowing, *Electron. Letters* 2004; 40: 992-993.
18. Report of European Nanoelectronics Initiative Advisory Council, Vision 2020 Nanoelectronics at the Centre of Change, June 2004, http://www.cordis.lu/ist/eniac/